Journal of Materials Chemistry C

Accepted Manuscript

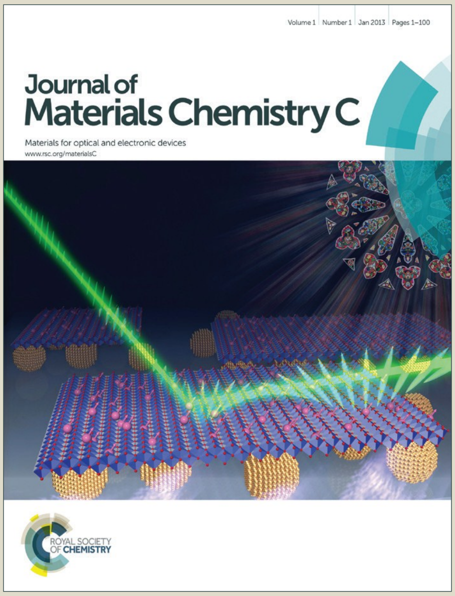

Volume 1 | Number 1 | Jan 2013 | Pages 1–100

Journal of Materials Chemistry C

Materials for optical and electronic devices

www.rsc.org/materialsC

ROYAL SOCIETY OF CHEMISTRY

ROYAL SOCIETY OF CHEMISTRY

www.rsc.org/materialsC

Journal Name RSCPublishing

COMMUNICATION

Cite this: DOI: 10.1039/x0xx00000x

Design of ceramic phosphor plate with functional materials for applications in high power LEDs

Eun-Kyung Ji[†a], Young-Hyun Song[†b], Sang Hwan Bak[†b], Mong Kwon Jung[c], Byung Woo Jeong[d] and Dae-Ho Yoon[*ab]

Received 00th January 2012,
Accepted 00th January 2012

DOI: 10.1039/x0xx00000x

www.rsc.org/

Here we report a ceramic phosphor plate made with different functional materials, such as SiO_2 and MgO, and $Lu_3Al_5O_{12}:Ce^{3+}$ (LuAG:Ce) for fabrication of remote phosphor in high-power LED applications. Remote phosphor can be applied directly to LEDs for thermal dissipation. The amounts of SiO_2 and MgO were controlled to optimize the photoluminescence (PL) intensities. Addition of MgO was more effective, and the optimized content of MgO was between 5 and 5.5 wt%. Ceramic phosphor plates with MgO showed better properties than others with regard to thermal stability, performance degradation and CIE colour coordinates changes. MgO is expected to be an effective functional material for the fabrication of ceramic phosphor plates.

White-light emitting diodes (LEDs) have been expected to bring about a revolution in solid state lighting technology, by replacing traditional lighting such as incandescent and fluorescent lamps with devices of superior energy efficiency while simultaneously advancing a growth industry for the implementation of a low-carbon green-growth society[1]. In recent years, LEDs have been introduced as new technology into a large pre-existing market for display technology and illumination. The white LEDs are based on fluorescent material, and a widely used method to manufacture a white LED involves combining a InGaN blue LED chip with a yellow phosphor in a package that is formed from a degassed mixture of a silicone resin, a curing agent and fluorescent materials[2,9]. However, in conventional processing the phosphor cannot be counted on to be uniformly dispersed in the syringe and it is difficult to implement the process consistently with the same white colour coordinate. Furthermore, since there is epoxy or silicone resin in the mix, the thermal stability and thermal conductivity of the cured material is not suitable for application in white LEDs and LED backlight units, both of which require a stable light output over a long period of time and high thermal conductivity of the package in order to minimize thermal aging[3,4,8]. Therefore, for high power and high efficiency in lamp applications, the phosphors of LEDs need to have a high thermal stability and a long life. An alternative to phosphor powders with silicone would be to develop a technology that substitutes a ceramic phosphor plate. It is an approach that can significantly resolve the problems of non-uniformity, resin deterioration, low thermal conductivity, colour reproducibility, light-transmittance, and packaging failure rates. Lumiramic, the new phosphor technology using polycrystalline ceramic plate, was introduced by Philips in 2008 in order to achieve color-consistent white light in high-power LEDs[9]. The ceramic plates have excellent thermal and mechanical properties and the packaging process is very easy and simple. In addition, less organic matter is used for the ceramic phosphor plate and the thermal conductivity is higher than that of the conventional paste. In the present study, in a high-temperature and high-humidity environment we fabricated light-emitting stable ceramic phosphor plates by adding functional materials such as SiO_2 and MgO to the LuAG:Ce phosphor in varying amounts—with a conceptually new frame package design for using a ceramic phosphor plate in a high-power LED[5-7,10]. The choice of functional materials in the LuAG:Ce phosphor yielded superior luminescence properties under blue light illumination. The LuAG:Ce ceramic phosphor plates were fabricated as shown in Fig. 1.

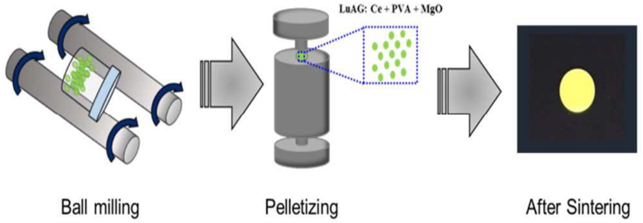

Figure 1. Illustration of procedure for fabrication of a LuAG: Ce ceramic phosphor plate

LuAG:Ce phosphors were made starting with a mixture of Lu_2O_3, Al_2O_3, and CeO_2, and AlF as the raw materials. The prepared powder was ground using an agate mortar for 30 min, horizontally loaded into a tubular alumina furnace with an inner diameter of 50 mm, and annealed at 1550 °C for 12 h under a reducing nitrogen atmosphere that contained 5% H_2 gas. The LuAG:Ce ceramic phosphor plate was fabricated with LuAG:Ce, PVA and functional materials such as SiO_2, and MgO. These materials were mixed and milled in a ball mill with ZrO_2 balls for 24 h with ethanol as a solvent. The mixture was then packed into disks and sintered at 1550 ºC for 6 h under a reducing nitrogen atmosphere containing 5% H2 gas. Samples of the LuAG:Ce ceramic phosphor plate were then polished to thicknesses varying from 90 to 160 µm. The surface morphology of the LuAG:Ce ceramic phosphor plate samples were observed by field-emission scanning electron microscopy (FE-SEM, JSM-7600F, JEOL). The crystalline phase of the LuAG:Ce phosphor was identified using powder X-ray diffraction (XRD, D-MAX 2500, Rigaku) with the CuKα target being aligned with $20° \leq 2\theta \leq 80°$. The optical properties of the prepared samples were analysed by room-temperature photoluminescence spectrometry (PL, PSI Co., Ltd./Korea), using a 500 W Xenon discharge lamp as an excitation source. Also, equivalent thermal properties of LuAG:Ce were measured based on a transient plane heat source (TPS) technique using the TPS2500 Thermal Conductivity System (Hot Disk AB, Sweden) which meets the ISO 22007-2:2008(E) standard. The measurement was conducted at room temperature within the measurement error of $\pm 2 \sim 5\%$.

Firstly, the XRD patterns of LuAG phosphor are indicated for confirmation of the exact phase in Fig. S1 (ESI†).

Fig. 2(a) shows the PL spectra under excitation at 450 nm with increasing amounts of SiO_2 (2, 4, 6, 8 and 10 %). The typical broad emission band shown at 530 nm with that excitation is ascribed to the electron transitions from the lowest crystal-field splitting component of the 5d level to the ground state of Ce^{3+} ($^2F_{5/2}$, $^2F_{7/2}$)[11,12]. With increasing SiO_2 content, the emission intensity was decreased. We suggest that the melted SiO_2 penetrates the space between the phosphor particles so that the ceramic phosphor plate is effectively vitrified at high temperatures. Fig. 2(b) also shows PL spectra but for SiO_2 concentrations of 1, 2, 3 and 4 %. Relative to the values for the pure sample, the emission intensity is gradually decreased as the SiO_2 concentration is increased. Fig. 2(c) gives PL emission intensities relative to that for the sample without SiO_2 as percentages, showing reductions with increasing SiO_2.

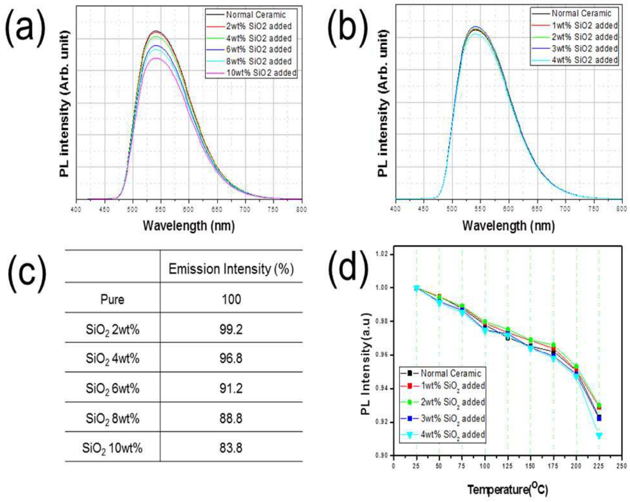

	Emission Intensity (%)
Pure	100
SiO_2 2wt%	99.2
SiO_2 4wt%	96.8
SiO_2 6wt%	91.2
SiO_2 8wt%	88.8
SiO_2 10wt%	83.8

Figure 2. (a) PL intensity of ceramic phosphor plate with SiO_2, (b) PL intensity for optimization of the SiO_2 concentration, (c) comparison of emission intensities, (d) PL intensity dependence on temperature.

Fig. 2(d) shows the temperature dependencies of the PL intensity for the ceramic phosphor plate samples with and without SiO_2 (with the data normalized to 1.0 at 25 ºC). With increasing the temperature up to 225 ºC, the relative PL intensity is decreased by up to about 9% compared to the initial value of the sample. In general, ceramic phosphor plate samples with SiO_2 had a lower PL intensity than the sample without SiO_2 because they showed higher thermal quenching stability. With these results, the addition of 2 wt% SiO_2 was confirmed to have strong temperature quenching properties at 225 ºC. It is due to the chemical and thermal stability and wide band-gap of SiO_2.

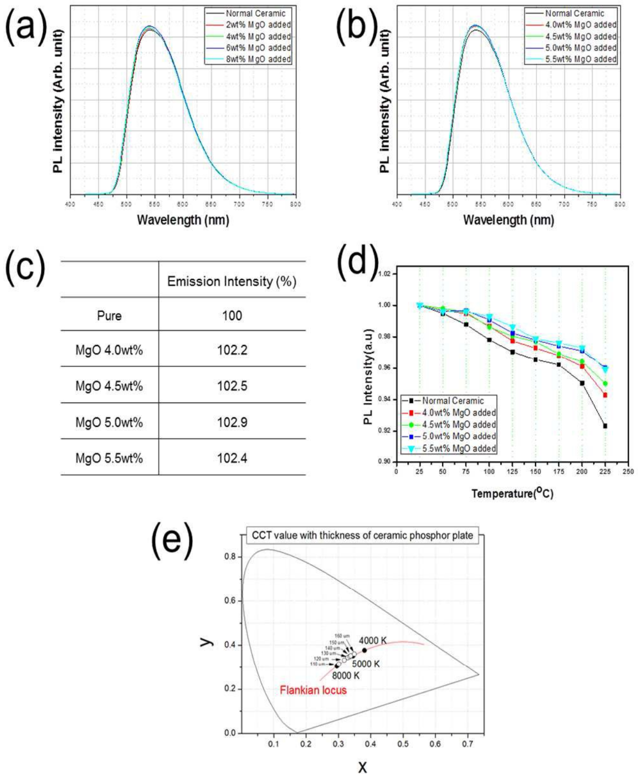

	Emission Intensity (%)
Pure	100
MgO 4.0wt%	102.2
MgO 4.5wt%	102.5
MgO 5.0wt%	102.9
MgO 5.5wt%	102.4

Figure 3. (a) PL intensity of ceramic phosphor plate with MgO, (b) PL intensity for optimization of the MgO concentration, (c) Comparison of emission intensities, (d) PL intensity dependence on temperature, (e) CIE colour coordinates for different of thicknesses.

The PL spectra as a function of MgO are shown in Fig. 3(a). The PL intensities increased with increasing amounts of MgO up to about 6 wt% and the highest intensities were shown by the samples with 4 and 6 wt% MgO. However, the emission intensity was degraded by the addition of 8 wt% MgO. For the optimization of the MgO concentrations in the ceramic phosphor plate, the functional materials were added at concentrations of from 4 to 5.5 wt% as shown in Fig. 3(b). There was no very noticeable difference among the emission intensities, but the highest emission intensity was observed at 5.0 wt% MgO. The values are shown in Fig. 3(c). PL intensities with different amounts of MgO as well as temperature changes from 25 ºC to 225 ºC were as shown in Fig. 3(d). The MgO addition definitely helped to alleviate thermal quenching. Considering the PL properties, the optimized amount of MgO is between 5 wt% and 5.5 wt%. Compared to the PL properties with SiO_2 added to the ceramic phosphor plate, PL intensities were better in the MgO-added ceramics. The MgO as functional materials between MgO and SiO_2 helps to eliminate the residual pores, preventing the abnormal grain growth. For applications in illumination, CIE colour coordinates were analysed with various thicknesses of the ceramic phosphor plate as shown in Fig. 3(e). With increasing thickness, lower CCT values are shown, which can be attributed to the absorption and emission of Ce^{3+} and the contents of the LuAG:Ce ceramic phosphor plate.

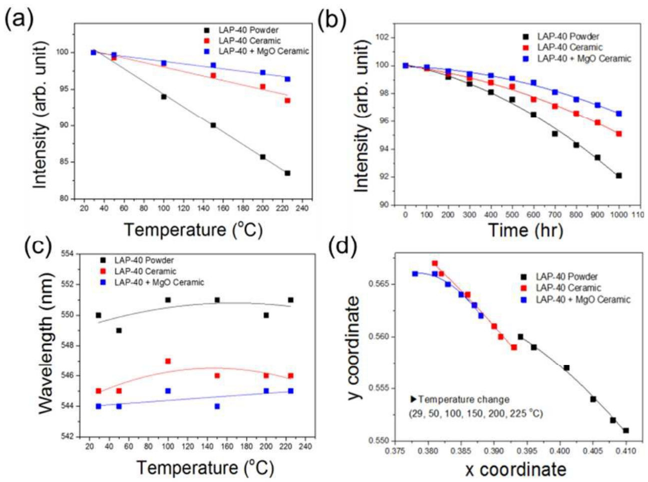

Figure 4. (a) Changes in PL intensity with temperature, (b) Reliability measurement at an elevated test temperature 85 ºC and a humidity of 85 % for 1000 h, (c) Change of wavelength with increasing temperature, (d) Differences in CIE colour coordinates as a function of sample.

In Fig. 4(a) shows changes in PL intensities versus temperature from 29 to 225 ºC. Comparing the phosphor powder, ceramic phosphor plate and ceramic phosphor plate to which MgO was added, the magnitudes of the changes in the PL intensities of the ceramics with temperature were observed to be in this order: phosphor powder > ceramic phosphor plate > ceramic phosphor plate with MgO. Intensities decrease to 85.7 %, 95.4 %, and 97.3% in the case of powder, ceramic without MgO and ceramic with MgO at 200 ºC, respectively. MgO is considered to be helpful to improve the thermal stability of the ceramic phosphor plate because the thermal resistivity of MgO is higher than that of other materials. Luminous properties degrade as time goes on, and phosphor powder is more vulnerable to degradation than ceramics. This is because the powder is in contact with the blue LED chip directly and is affected by heat generation from the blue LED chip. The degradation of the properties of the powder, ceramic phosphor plate and ceramic phosphor plate with MgO were measured at an elevated test temperature of 85 ºC and a humidity of 85 % for 1000 h as shown in Fig. 4(b). For the powder, ceramic phosphor plate and ceramic phosphor plate with MgO, the decreased emission intensities were measured as 92.1 %, 95.1 % and 96.6 %, respectively. This is because MgO reduces the residual pores, which trap the heat. Fig. 4(c) and (d) indicate the changes of emission wavelength and CIE colour coordinates as a function of temperature[13,14]. The ceramic phosphor plate with MgO shows a blue-shifted emission wavelength. The blue light from the blue LED chip was transmitted and reflected more with increased amounts of MgO, inducing the blue shift of the emission wavelength. The CIE colour coordinates deviation is also alleviated in the case of MgO-added ceramic. Fig. 5 shows thermal conductivities of powder, ceramic and MgO-added ceramic. Heat is conducted by phonons in non-metallic solids, and thermal conductivity is related to the mean free path of phonons. Thermal conductivity is proportional to the mean free path[15]. Porosity acts as a main factor of thermal conductivity, because it increases the degree of phonon scattering and lower the mean free path. As mean free path decreases, thermal conductivity also decreases. MgO helps to reduce the porosity, which increases thermal conductivity.

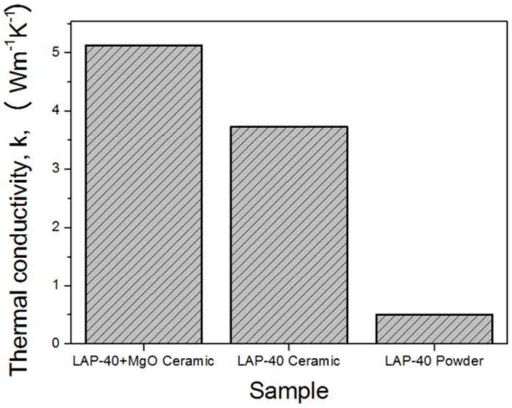

Figure 5. Thermal conductivity as a function of sample condition.

Table S1 (ESI†) summarizes the characteristics in LuAG:Ce ceramic phosphor plate.

In summary, we fabricated a LuAG:Ce ceramic phosphor plate containing functional materials. SiO2 was not helpful to improve the luminescent properties and it even lowers the PL intensities; MgO enhanced luminescence properties. A LuAG:Ce ceramic phosphor plate with MgO showed thermal stability compared to the others and the optimized amount of MgO was between 5 and 5.5 wt%. And 5 wt% MgO-added ceramic maintained its properties under heat and humidity better than others. We also analysed CCT values and CIE colour coordinates of the optimized ceramic phosphor plate as a function of thickness, and CCT decreased with increasing thickness. We suggest that MgO can act as an effective functional material for the next-generation high-power LEDs.

This research was supported by Basic Science Research Program through the National Research Foundation of Korea (NRF) funded by the Ministry of Education, Science and Technology (NRF- 2013R1A2A2A01010027).

Notes and references

[a] SKKU Advanced Institute of Nanotechnology (SAINT), Sungkyunkwan University, Suwon 440-746, Republic of Korea. *Email: dhyoon@skku.edu
[b] School of Advanced Materials Science & Engineering, Sungkyunkwan University, Suwon 440-746, Republic of Korea
[c] Hyosung Corporation, R&D Business Labs, Anyang 431-080, Republic of Korea
[d] LG Electronics, Future Device R&D Department, Seoul 137-724, Korea
† These authors contributed equally to this work.

1 Daniel A. Steigerwald, Jerome C. Bhat, Dave Collins, Robert M. Fletcher, Mari Ochiai Holcomb, Michael J. Ludowise, Member, IEEE, Paul S. Martin, and Serge L. Rudaz, *IEEE J. Sel. Topics Quantum Electron.*, 2002, 8, 310.
2 S. Fujita, A. Sakamoto, and S. Tanabe, *IEEE J. Sel. Topics Quantum Electron.*, 2008, 14, 1387.
3 N. Narendran, Y. Gu, J.P. Freyssinier, H. Yu, and L. Deng, *J. Cryst. Growth.*, 2004, 268, 449.
4 S. Nishiura, S. Tanabe, K. Fujioka, and Y. Fujimoto, *Opt. Mater.*, 2011, 33, 688.
5 H. Yang, X. Qin, J. Zhang, J. Ma, D. Tang, S. Wang, and Q. Zhang, *Opt. Mater.*, 2012, 34, 940.
6 H. Yang, X. Qin, J. Zhang, S. Wang, J. Ma, L. Wang, and Q. Zhang, *J. Alloy. Compd.*, 2011, 509, 5274.
7 M. Stuer, P. Bowen, M. Cantoni, C. Pecharroman, and Z. Zhao, *Adv. Funct. Mater.*, 2012, 22, 2303.
8 S.W. Yoon, H.K. Park, K.Y. Ko, J. Ahn, and Y.R. Do, *J. Mater. Chem. C.*, 2014, 2, 7513.
9 H. Bechtel, P. Schmidt, W. Busselt, B.S. Schreinemacher, *Proc. Of SPIE*, 2008, 7058, 70580E-1.
10 H.L. Li, X.J. Liu, and L.P. Huang, *J. Am. Ceram. Soc.*, 2005, 88, 3226.
11 D. Haranath, H. Chander, P. Sharma, and S. Singh, *Appl. Phys. Lett.*, 2006, 89, 173118.
12 M. Raukas, S.A. Basun, W. van Schaik, W.M. Yen and U. Happek, *Appl. Phys. Lett.*, 1996, 69, 3300.
13 Y. Li, S. Zhou, H. Lin, X. Hou, W. Li, H. Teng, and T. Jia, *J. Alloy. Compd.*, 2010, 502, 225.
14 P.J. Jorgensen, J.H. Westbrook, *J. Am. Ceram. Soc.*, 1964, 47, 332.
15 K.T. Regner, D.P. Sellan, Z. Su, C.H. Amon, A.J.H. McGaughey, and J.A. Malen, *Nat. Commun.*, 2013, 4, 2630.